Electronic Supplementary Material (ESI) for RSC Advances.

Supporting Information 1 (SI1)

Upconverting/magnetic: Gd_2O_3:(Er^{3+},Yb^{3+},Zn^{2+}) nanoparticles for biological applications: Effect of Zn^{2+} doping

Izabela Kamińska, Krzysztof Fronc, Bożena Sikora, Matthew Mouawad, Aleksander Siemiarczuk, Maciej Szewczyk, Kamil Sobczak, Tomasz Wojciechowski, Wojciech Zaleszczyk, Roman Minikayev,Wojciech Paszkowicz, Piotr Stępień, Piotr Dziawa, Kamil Ciszak, Dawid Piątkowski, Sebastian Maćkowski, Miron Kaliszewski, Maksymilian Włodarski, Jarosław Młyńczak, Krzysztof Kopczyński, Mariusz Łapiński and Danek Elbaum*

1. Experimental section

1.1 Synthesis of NPs

For the preparation of Gd_2O_3:(Er,Yb,Zn) NPs we applied a microwave-induced solution combustion synthesis (Fig. S1a). Stoichiometric amounts of substrates were used for the production process. Urea (Sigma Aldrich) was used as a reducer and nitrates of gadolinium, erbium, ytterbium (Sigma Aldrich) and zinc (Chempur), as oxidants. The mixture chemical compositions were summarized in Table S1.

Subsequently the mixtures were dissolved in a minimum amount (20 ml) of deionized water and the resulting solution was warmed in a microwave oven to 500 °C (750 W). During the reaction the evaporation of water, frothing of the mixture and spontaneous combustion took place (Fig. S1b, c, d). The resulted fluffy mass (Fig. S1e) was grounded in an agate mortar to obtain a powder (Fig. S1f). We obtained six samples of gadolinium oxide Gd_2O_3 NPs doped with Er^{3+}, Yb^{3+} containing various concentrations of Zn^{2+} (Fig. S1g). The resulting material was calcined in a furnace in the air atmosphere at 900 °C for 2 h. In order to separate the NPs from each other, during the MiSCs synthesis, 3 mM, 6 mM, 8 mM and 11 mM of NaCl was added.[1] The molar ratio of NaCl ions to the metal ions used in the reaction was 0.6 . After the combustion process NaCl was removed by dissolution in water.

1.2 Coating with PVP

Samples of the Gd_2O_3:(Er,Yb,Zn) NPs (1.4 g) was dissolved in 40 ml of ethanol. 0.5 mmol of a PVP polymer (polyvinylpyrrolidone) was dissolved in 20 ml of ethanol. Then both solutions were mixed, stirred and heated at 45 °C. This temperature was maintained for 6 h. The solution was next cooled down to room temperature, centrifuged at 22 °C for 15 min at a speed of 6000 rpm and subsequently dried at a temperature of 60 °C.

1.3 Absolute quantum yield measurements

The absolute quantum yield was measured using a spectrofluorimeter QuantaMaster-40 from Horiba – PTI with an extended Hamamatsu R2658 photomultiplier (180 nm – 1010 nm) equipped with an integrating sphere (Fig. S2) and SDL-980-LM-1000MFL laser (Shanghai Dream Lasers). Measurements were made at 597.7 mW, 289.7 mW, 207.4 mW, 68.3 mW, 58.3 mW, 42 mW, 37.6 mW, 20.5 mW, 14.7 mW, which correspond to a laser power densities: 19 $W \cdot cm^{-2}$, 9.2 $W \cdot cm^{-2}$, 6.6 $W \cdot cm^{-2}$, 2.2 $W \cdot cm^{-2}$, 1.9 $W \cdot cm^{-2}$, 1.3 $W \cdot cm^{-2}$, 1.2 $W \cdot cm^{-2}$, 0.7 $W \cdot cm^{-2}$ and 0.5$\cdot$W cm^{-2}. Illuminated spot had diamater of approximately 2 mm. Neutral density attenuating filters were used for varying the power of the excitation.

1.4 Photoluminescence

The photoluminescence (PL) spectra in the visible (VIS) and in the infrared (IR) regions were measured with a Jobin Yvon-SPEX 270 M monochromator. The excitation (λ_{exc} = 980 nm) source was an IR laser diode (Lumics model LU0980D300-DNA014). For the measurement of PL in the VIS region from 500 nm to 700 nm, Shortpass Filter FES0700 (Thorlabs) was applied. Longpass Filter FEL1000 (Thorlabs) was used for measurement of luminescence in the IR range (1000 nm – 1060 nm). Powdered samples were measured by placing them in-between two quartz slides. PL of NPs was also measured in dimethyl sulfoxide (DMSO). Solution (0.02 $mg\cdot ml^{-1}$) sample with 5 % Zn^{2+} was sonicated in an ultrasonic scrubber for 15 minutes, and then measured in a 3 ml quartz cuvette.

1.5 Luminescence decay and luminescence maps

In the experiment we used scanning confocal microscope based on the Nikon Eclipse Ti-s microscope body. The microscope was equipped with high numerical aperture objective (Nikon 60x NA 1.4 OIL) and an infrared 1 mW laser operating at 980 nm. Samples were mounted on a piezo-electric stage (PI-517, Physik Instrumente) operating with resolution of about 10 nm. The detection of emission was carried out with an avalanche photodiode (SPCM-AQRH-14, PerkinElmer) and a set of band pass filters (550/40 nm, 650/30 nm, Chroma) dedicated for Er^{3+} emission lines as well as 2P BS 780 DCSPXR dichroic mirror. For time-resolved experiments we used MSA-300 multiscaler card (Becker&Hickl) and function generator (Keithley 3390) which served as a trigger source. For spectrally-resolved measurements we used Shamrock SR-500 (Andor) monochromator coupled with EMCCD camera (Newton 970, Andor). The spatial resolution of the microscope set-up was about 500 nm.

1.6 Excitation-emission maps

The experimental setup used for the excitation-emission NPs measurements was shown in Fig. S3. The sample (powdered) was placed between holder and a thin quartz window. The sample was excited by a Tunable Nd:YAG-Laser System NT342B-10 (EXPLA). Emission spectrum was collected via a fiber connected to CCD spectrometer. The FES0700-1 (Thorlabs) filter was used to cut off the laser excitation line from collected spectra. The excitation power of the laser was monitored during the experiment by diverting 10% of the beam to the power meter.

Excitation source

Tunable Nd:YAG-Laser System NT342B-10 comprises of a pump laser NL300, harmonics generators (SHG, THG) and optical parametric oscillator (OPO).

Measurements

The samples were excited in the range of 900 nm – 1002 nm with the 3 nm steps. The emission spectra were recorded in a range from 286 nm to 840 nm with 0.3 nm steps. Each spectrum was averaged from the spectra resulting from 10 excitation impulses. During the measurements the energy of laser pulses was measured for spectral correction.

1.7 Magnetic properties

Magnetic properties were studied using Superconducting Quantum Interference Device (SQUID) magnetometer at temperatures from 5 K to 200 K. Measurements of magnetization as a function of temperature, both zero-field-cooled (ZFC) and field-cooled (FC) regimes were carried out at applied external magnetic field of 10 Oe as well as magnetic field dependence at T = 5 K.

1.8 Toxicity tests

At the first stage the NPs were sonicated for 20 minutes. Then the transfection mixture was prepared by diluting solutions of the particles in a sterile ddH_2O to a final concentration of 0.5, 1, 5, 10, and 50 $\mu g \cdot ml^{-1}$ and by adding the transfection reagent (Invitrogen Lipofectamine 2000; 20 µl/1.5 ml of particle mixture). The mixtures were incubated for 20 minutes at room temperature. Meanwhile, HeLa cells were washed with phosphate buffer saline (PBS) pH 7,4 and detached by 10 min incubation with 0.025% Trypsin-EDTA (Sigma) at 37 °C. Trypsin was neutralized by addition of fresh medium supplemented with 10% fetal bovine serum. Cells were counted in Thoma chamber and diluted to final concentration of 10^5 ml^{-1}. 10 µl of transfection solution and 90 µl of cell suspension (approx. 9000 cells) were added per well of a 96-well plate in an automatic Janus pipetting workstation (Perkin Elmer). Cells were incubated at 37 °C for 24 h or 48 h. Then, 10 µl/well of PrestoBlue reagent (Invitrogen) was added. After 30 min incubation in darkness at 37 °C fluorescence of PrestoBlue (excitation 540 nm, emission 590 nm) was measured in Paradigm microplate reader (Beckmann Coulter).

1.9 Cell culture and laser scanning upconversion luminescence microscopy imaging in vitro

The Er^{3+}, Yb^{3+} and Zn^{2+} doped gadolinium oxide NPs were introduced into HeLa cells, using the previously reported procedure Kamińska *et al.*[2] . Transfection agent (Lipofectamine 2000) was used to introduce the NPs into the cells. The cells were cultured in 6 well plates (6×10 cm^2) at a density of 10^5 per plate. The cells were incubated with the Gd_2O_3:1% Er^{3+},18% Yb^{3+},50% Zn^{2+}/PVP NPs and with the transfection agent. Solutions were prepared with varying concentration of particles: 1 $\mu g \cdot ml^{-1}$, 25 $\mu g \cdot ml^{-1}$, 40 $\mu g \cdot ml^{-1}$ and 50 $\mu g \cdot ml^{-1}$ and then incubated with HeLa cells for different times: 4 h, 10 h, 24 h. Then, the cells were fixed by filtered paraformaldehyde. Bioimaging of HeLa cells, incubated with the Gd_2O_3:1% Er^{3+},18% Yb^{3+},50% Zn^{2+}/PVP NPs, was performed using a commercial Confocal Laser Scanning Microscope (Zeiss 710 NLO) with a NIR femtoseconds laser (Coherent, Chameleon). The samples were excited by a 980 nm and two visible UC emission channels were detected at green (507 nm – 585 nm) and red (620 nm – 710 nm) spectral regions. Autofluorescence of HeLa cells was observed when excited at 488 nm with an argon laser and detected at 508 nm – 585 nm.

1.10 Powder X-ray Diffraction

X-ray diffraction was applied for evaluation Gd_2O_3:(Er,Yb,Zn) NPs (powdered) crystal structure and size. NPs were investigated using a Philips X´Pert Pro Alpha1 MPD diffractometer (Panalytical) (λ = 1.5406 Å).

1.11 Transmission Electron Microscopy

The study was performed using transmission electron microscope JEOL JEM 2000EX operating at 200 kV. Images were recorded on photographic plates, and then using a scanner Nikon LS-8000 were processed into digital form for further analysis. Observations were performed using diffraction contrast techniques: the bright-field (image forming with the incident beam) and the dark-field (image forming with a diffracted beam).

1.12 Scanning Electron Microscopy

SEM was used to assess the NPs surface morphology. In addition, EDX measurements were performed to confirm the presence of the elements in the tested samples.

Table S1. Summary of the obtained materials.

	Mass of reducer	Mass of oxidants			
The content of Zn^{2+} in relation to the amount of Gd^{3+} in the starting material Gd_2O_3: 1% Er^{3+}, 18% Yb^{3+} (%)	Urea $CO(NH_2)_2$ (Sigma Aldrich) (g)	Gadolinium nitrate -$Gd(NO_3)_3 \times 6H_2O$, (Sigma Aldrich) (g)	Erbium nitrate - $Er(NO_3)_3 \times 6H_2O$, (Sigma Aldrich) (g)	Ytterbium nitrate - $Yb(NO_3)_3 \times 6H_2O$, (Sigma Aldrich) (g)	Zinc nitrate - $Zn(NO_3) \times 6H_2O$, (Chempur) (g)
0	4.76	4.9	0.026	0.48	-
2.5	4.91	4.9	0.026	0.48	0.09
5	5.03	4.9	0.026	0.48	0.18
20	5.75	4.9	0.026	0.48	0.71
25	5.99	4.9	0.026	0.48	0.89
50	7.19	4.9	0.026	0.48	1.78

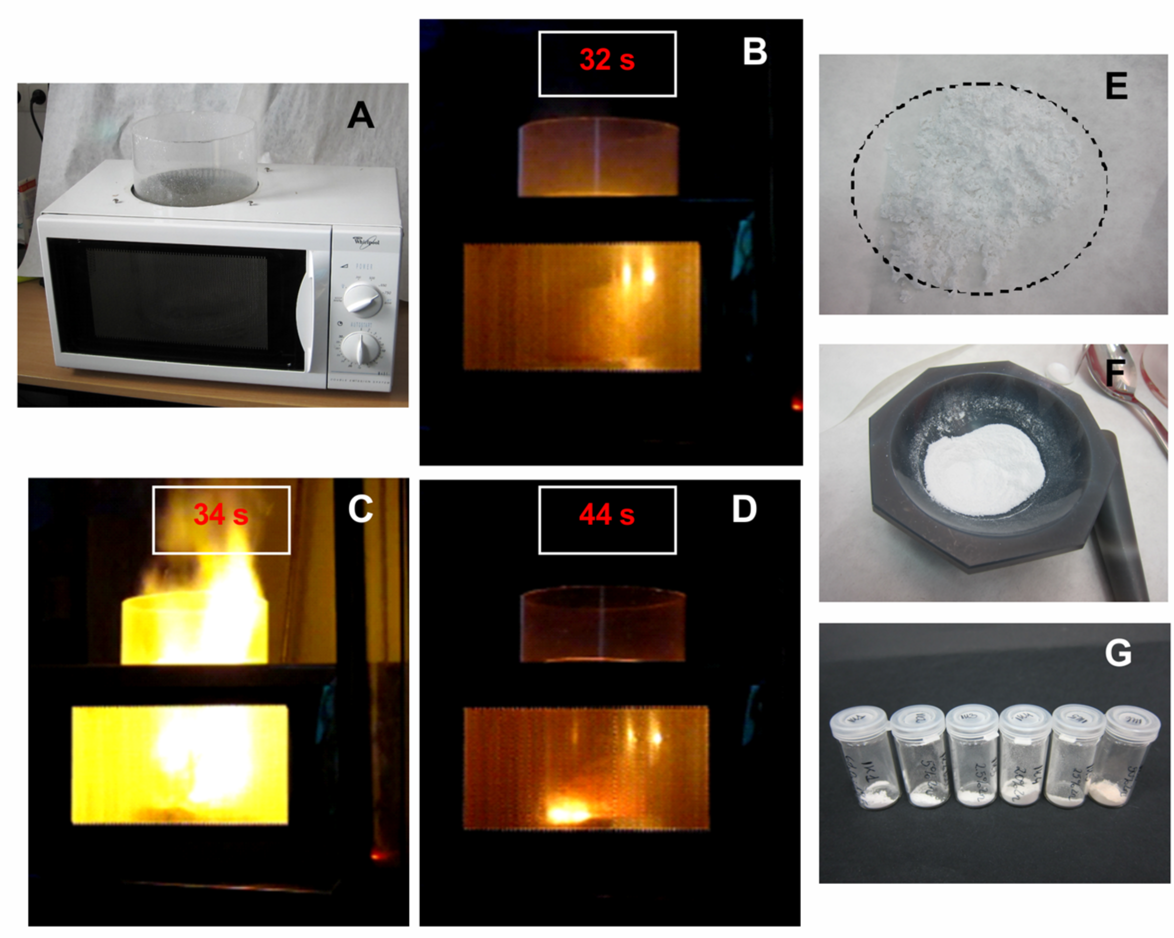

Fig. S1 A) Microwave oven used for high-temperature synthesis of Gd_2O_3 NPs doped with Er^{3+}, Yb^{3+} and Zn^{2+}. Combustion synthesis procedure in a microwave oven over time: B) 32 s C) 34 s D) 44 s. E) Fluffy mass directly received after synthesis. F) The nanoparticles milled in an agate mortar. G) The resulting NPs samples.

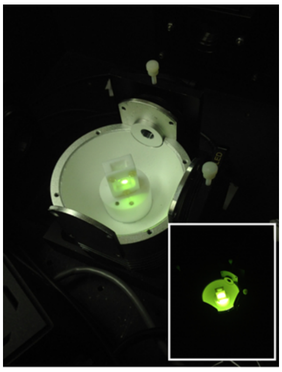

Fig. S2 Photos of the integrating sphere with illuminated sample by the 980 nm laser.

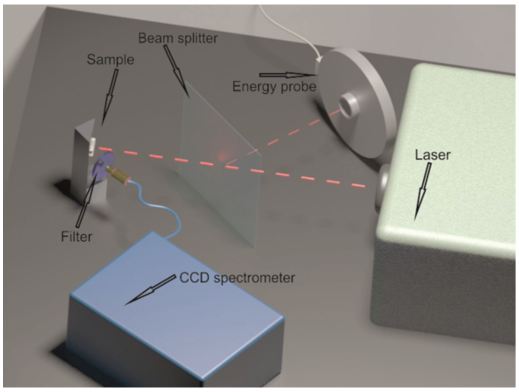

Fig. S3 Scheme of the experimental setup used for excitation-emission NPs measurements.

1.13 Reproducibility testing of Gd_2O_3: 1% Er^{3+}, 18% Yb^{3+} and Gd_2O_3 : 1% Er^{3+}, 18%Yb^{3+}, 5% Zn^{2+} nanoparticles

In the Institute of Physics PAS (IP PAS) we examined cell parameter of Gd_2O_3: Er^{3+}, Yb^{3+} nanoparticles for 1 and 2 samples. Whereas measurements at the third sample was carried out at the Institute of Ceramics and Building Materials (ICBM) (Fig. S4). The samples were investigated using a Philips X´Pert Pro Alpha1 MPD diffractometer (Panalytical) (λ = 1.5406 Å) (IP PAS) and X-ray diffractometer D8 DISCOVER (ICBM).

In the first case, in order to examine the structural parameters of the samples, Rietveld refinement was performed. In the case of the 3 samples measured in the ICBM, we determined structural parameters using Pawley refinement, after earlier determination of widening reflections and the other constant parameters of X-ray beam, on the pattern NIST number 660b (LaB_6).

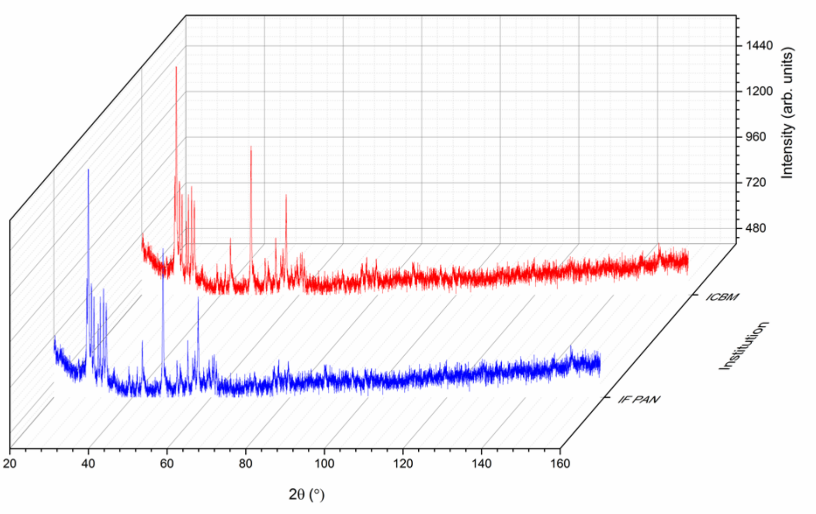

Fig. S4 Diffractograms obtained for the two samples Gd_2O_3: Er^{3+}, Yb^{3+} nanoparticles measured in the IP PAS and ICBM.

Table S2. Cell parameters obtained Gd_2O_3: Er^{3+}, Yb^{3+} nanoparticles.

	Sample 1	Sample 2	Sample 3
Phase	IF PAS	IF PAS	ICBM
		(Å)	
Gd_2O_3 (C2/m)	a = 14.07254 ± 0.00030	a = 14.06999 ± 0.00028	a = 14.1022(41)
	b = 3.56318 ± 0.00007	b = 3.56038 ± 0.00005	b = 3.5529(16)
	c = 8.74296 ± 0.00021	c = 8.73932 ± 0.00020	c = 8.74420(12)
	β = 100.23065 ± 0.00159	β = 100.2439 ± 0.00158	β = 100.232(23)
Gd_2O_3 (Ia-3)	a = 10.78165 ± 0.00019	a = 10.77445 ± 0.00021	a = 10.7797(12)

The obtained lattice parameters from the XRD measurements have a similar values as demonstrated by the data collected in Table S2. Thus we can conclude that, as a results of the synthesis, we obtained repeatable samples.

The second experiment which we conducted in order to check whether our results are reproducible, was to determine emission spectra of Gd_2O_3: 1% Er^{3+}, 18%Yb^{3+}, 5% Zn^{2+} nanoparticles, in the visible region, by 980 nm excitation. The measurements were performed on 3 samples, under identical geometrical conditions of the optical system, and under identical values of the excitation power densities.

As shown on Fig. S5 the emission spectra of the three tested samples are reproducible. These nanoparticles exhibit luminescence at a maximum wavelength of 550 nm and 660 nm. As judged by the total areas under the emission spectra, for the three independent samples, the quantum yields are comparable Table S3.

Thus, based on the structural similarities (X-ray) of three zinc free samples and spectroscopic properties of Zn containing samples (emission), the synthesis methodology is reproducible.

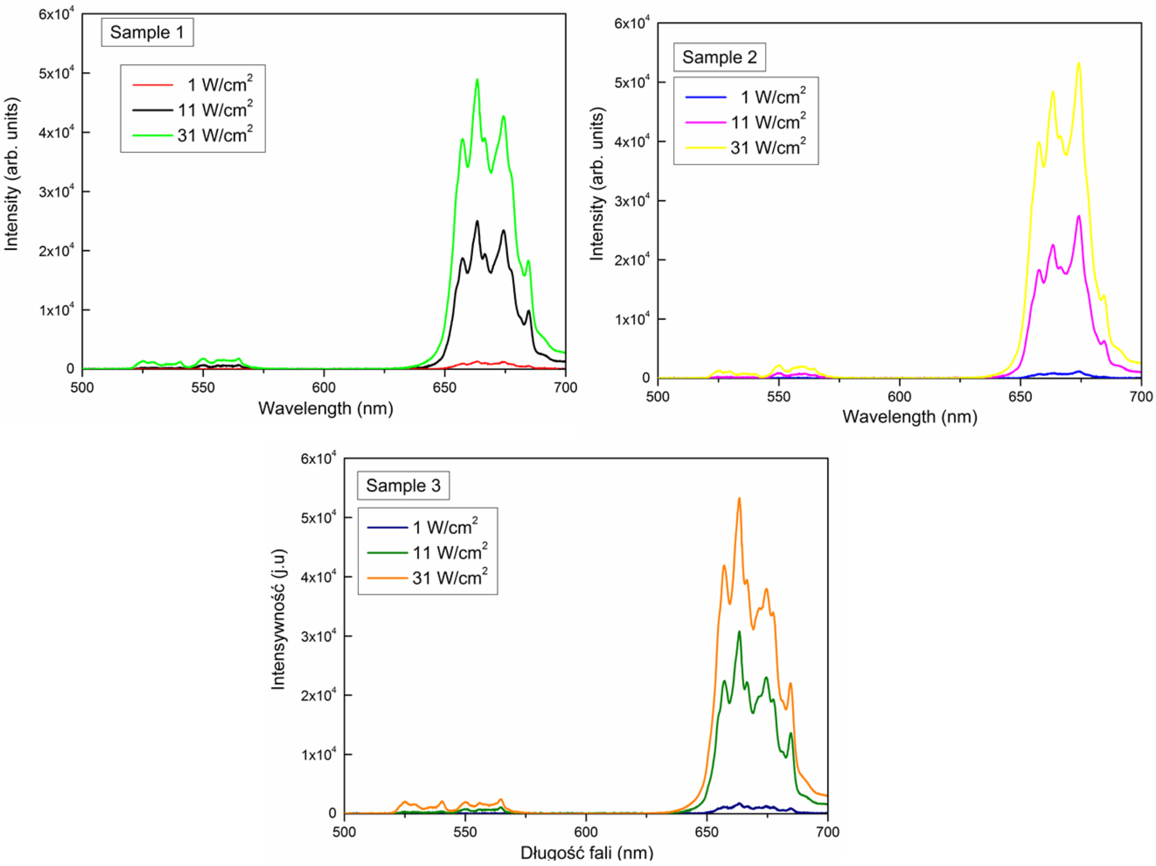

Fig. S5. Emission spectra of the three tested samples of Gd_2O_3: 1% Er^{3+}, 18%Yb^{3+}, 5% Zn^{2+} nanoparticles measured at different a laser power densities of 980 nm.

Table S3. Relative number of photons emitted and obtained from Gd_2O_3: 1% Er^{3+}, 18%Yb^{3+}, 5% Zn^{2+} nanoparticles.

	Relative number of photons (arb. units)									
Power density (W/cm^2)	**Sample 1**			**Sample 2**			**Sample 3**			
	I_{green}	I_{red}	I_{red}/ I_{green}	I_{green}	I_{red}	I_{red}/ I_{green}	I_{green}	I_{red}	I_{red}/ I_{green}	Average I_{red}/ I_{green}
1	-	30747	-	-	22106	-	-	36161	-	-
11	15355	590225	38	16740	577879	35	19455	676072	35	36,0 ± 1,7
31	52769	1205207	23	54668	1251759	23	55883	1232949	22	22,6 ± 0,3

1.14 Safety statement with the description of the microwave

All experiments involving the microwave-induced solution combustion synthesis were performed maintaining required safety standards.

We used a modified Whirlpool Microwave Model AVM/401/1/WH. The modification consisted of cutting out a hole in the upper wall in order to discharge gases produced during the synthesis (Fig. S6a). The chimney made of quartz glass was inserted through the hole (Fig. S6a). Microwave were controlled by additional control panel placed at a distance of about 5 m from the device (Fig. S6b).

In addition, a stainless steel mesh cap (Fig. S7a) was placed above the hole. The device was placed inside a chemical fume hood (Picture S6c). In addition, to limit the level of microwave radiation escape, a "cage" made of copper mesh (1 mm mesh diameter) attached to the hood was constructed (Fig. S6c, Fig. S7b). The level of radiation was investigated using a Microwave Leakage Detector and determined to be less than 0.1 mW/cm^2 at a distance of 5 meters from the device.

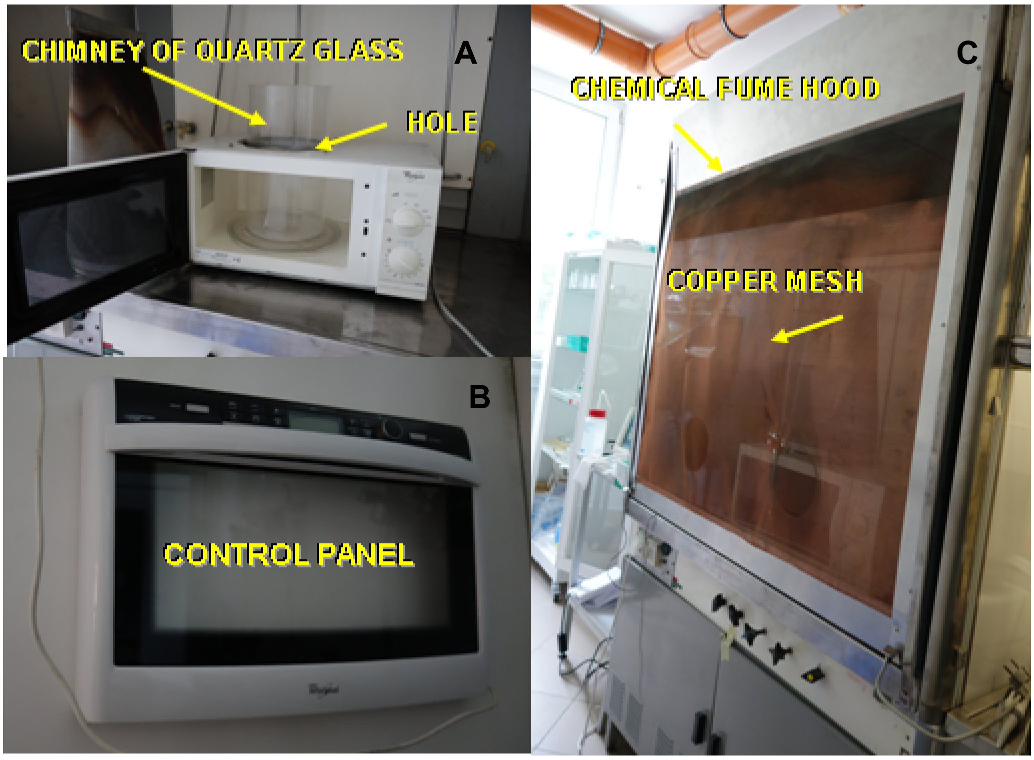

Fig. S6. A) A modified Whirlpool Microwave Model AVM/401/1/WH. B) The control panel. C) A chemical fume hood with a "cage" made of copper mesh.

Fig. S7. A) A stainless steel mesh cap and B) view of valve a chemical fume hood in front.

Table S4. Parameter of the crystal lattice.

	Phase Gd_2O_3: 1% Er^{3+}, 18% Yb^{3+}, x% Zn^{2+}									
x% Zn^{2+} (non-calcined)	**Monoclinic**					**Cubic**		**ZnO (hexagonal)**		
	a(Å)	**b(Å)**	**c(Å)**	**β**	**%**	**a(Å)**	**%**	**a(Å)**	**c(Å)**	**%**
0	14.07254 ± 0.00030	3.56318 ± 0.00007	8.74296 ± 0.00021	100.23065 ± 0.00159	60.16 ± 0.45	10.78165 ± 0.00019	39.84 ± 0.35	-	-	-
2.5	14.07006 ± 0.00025	3.56142 ± 0.00006	8.74077 ± 0.00017	100.19921 ± 0.00128	64.22 ± 0.35	10.77948 ± 0.00014	35.78 ± 0.24	-	-	-
5	14.06794 ± 0.00024	3.56097 ± 0.00006	8.73979 ± 0.00016	100.20696 ± 0.00112	53.48 ± 1.74	10.77814 ± 0.00015	46.52 ± 1.63	-	-	-
20	14.06979 ± 0.00027	3.56096 ± 0.00007	8.74054 ± 0.00019	100.20031 ± 0.00125	81.19 ± 0.52	10.77839 ± 0.00024	18.81 ± 0.27			
25	14.06915 ± 0.00031	3.56074 ± 0.00007	8.73994 ± 0.00021	100.22092 ± 0.00137	80.56 ± 0.55	10.77704 ± 0.00026	19.44 ± 0.27			
50	14.07286 ± 0.00045	3.56147 ± 0.00010	8.74185 ± 0.00030	100.23469 ± 0.00202	66.34 ± 0.67	10.77936 ± 0.00032	24.15 ± 0.40	3.25001 ± 0.00021	5.20434 ± 0.00055	9.51 ± 0.22
x% Zn^{2+} (calcined)	**Monoclinic**					**Cubic**		**ZnO hexagonal**		
	a(Å)	**b(Å)**	**c(Å)**	**β**	**%**	**a(Å)**	**%**	**a(Å)**	**c(Å)**	**%**
0	14.07063 ± 0.00054	3.56143 ± 0.00013	8.74109 ± 0.00039	100.22256 ± 0.00346	26.91 ± 0.59	10.77750 ± 0.00011	73.09 ± 0.59	-	-	-
2.5	14.07226 ± 0.00082	3.56165 ± 0.00021	8.74176 ± 0.00055	100.21375 ± 0.00288	41.99 ± 0.69	10.78053 ± 0.00037	58.01 ± 0.66	-	-	-
5	14.07476 ± 0.00073	3.56124 ± 0.00019	8.74202 ± 0.00049	100.23383 ± 0.00269	42.96 ± 0.64	10.77890 ± 0.00039	57.04 ± 0.58	-	-	-
20	14.07621 ± 0.00036	3.56089 ± 0.00009	8.74247 ± 0.00024	100.25504 ± 0.00134	43.47 ± 0.33	10.77959 ± 0.00020	55.49 ± 0.30	3.25127 ± 0.00007	5.20284 ± 0.00018	1.04 ± 0.07
25	14.07885 ± 0.0002	3.56079 ± 0.00005	8.74279 ± 0.00013	100.27840 ± 0.00087	65.70 ± 0.36	10.77883 ± 0.00009	32.75 ± 0.20	3.25057 ± 0.00005	5.20590 ± 0.00013	1.55 ± 0.09
50	14.07754 ± 0.00071	3.56083 ± 0.00018	8.74286 ± 0.00049	100.26948 ± 0.00370	29.94 ± 0.62	10.77883 ± 0.00029	65.13 ± 0.67	3.25062 ± 0.00005	5.20318 ± 0.00012	4.93 ± 0.15

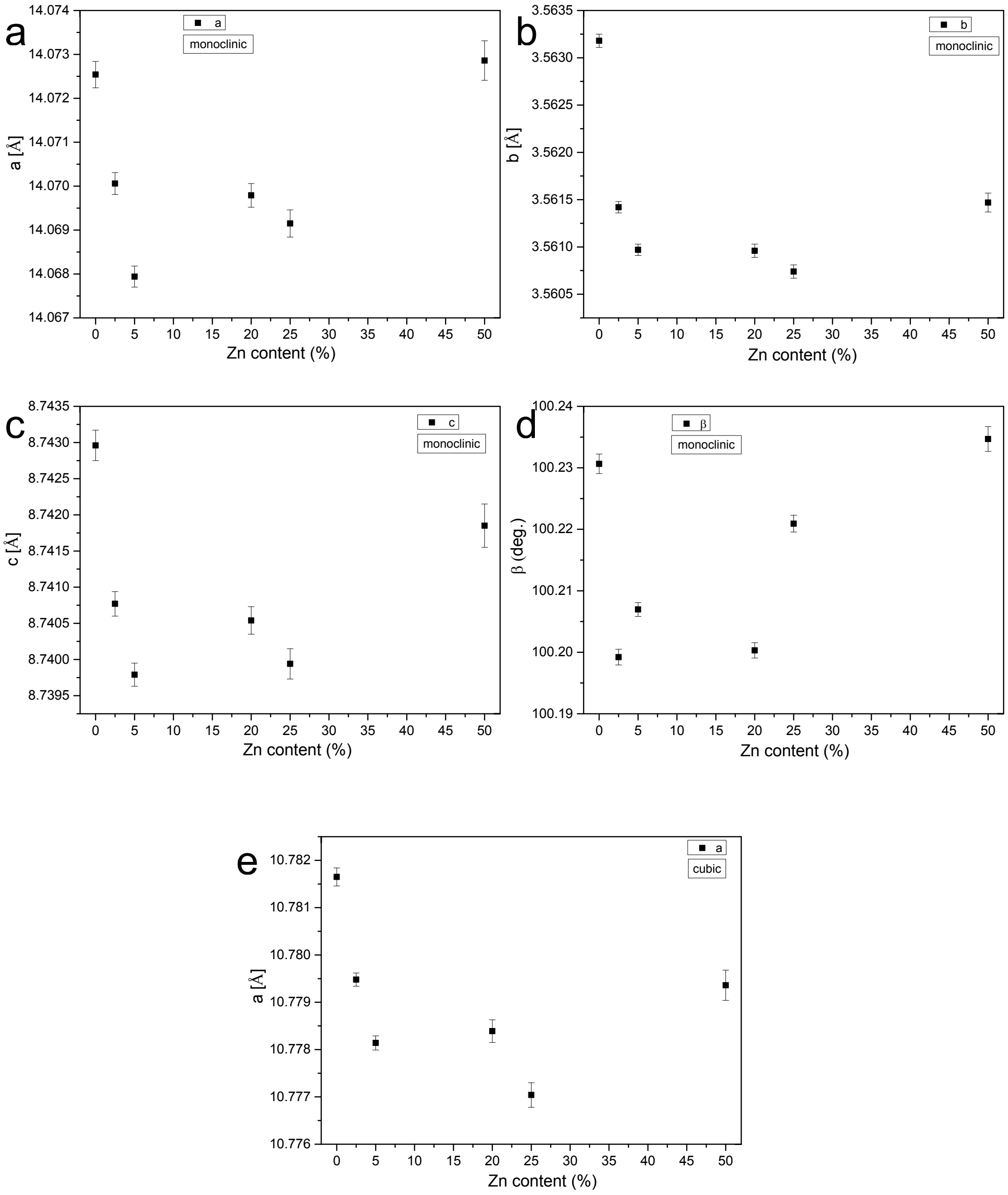

Fig. S8 Unit cell lattice constant of the Gd_2O_3 nanoparticles doped 1% Er^{3+}, 18% Yb^{3+} with different input Zn^{2+} content (A, B, C, D) monoclinic phase and E) cubic phase.

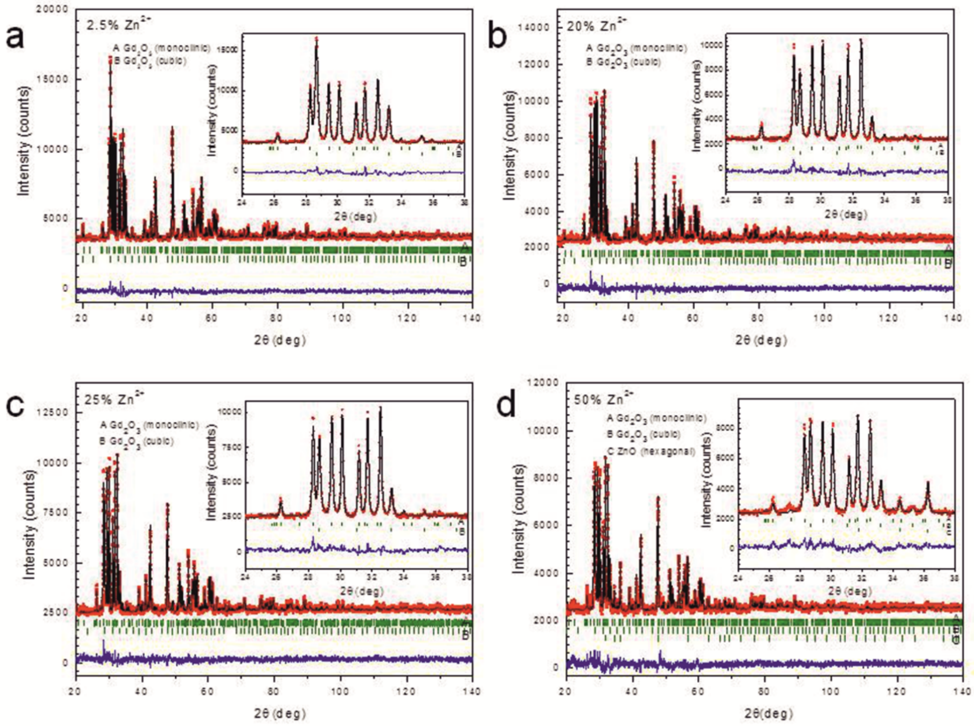

Fig. S9 Refinement of non-calcined NPs with various input concentrations of Zn^{2+} A) 2.5% B) 20% C) 25% and D) 50% by the Rietveld method. Symbols: experimental diffractogram (red points), theoretical (black line), differential curve (blue line), positions of Bragg reflection (green symbol).

Transmission Electron Microscopy

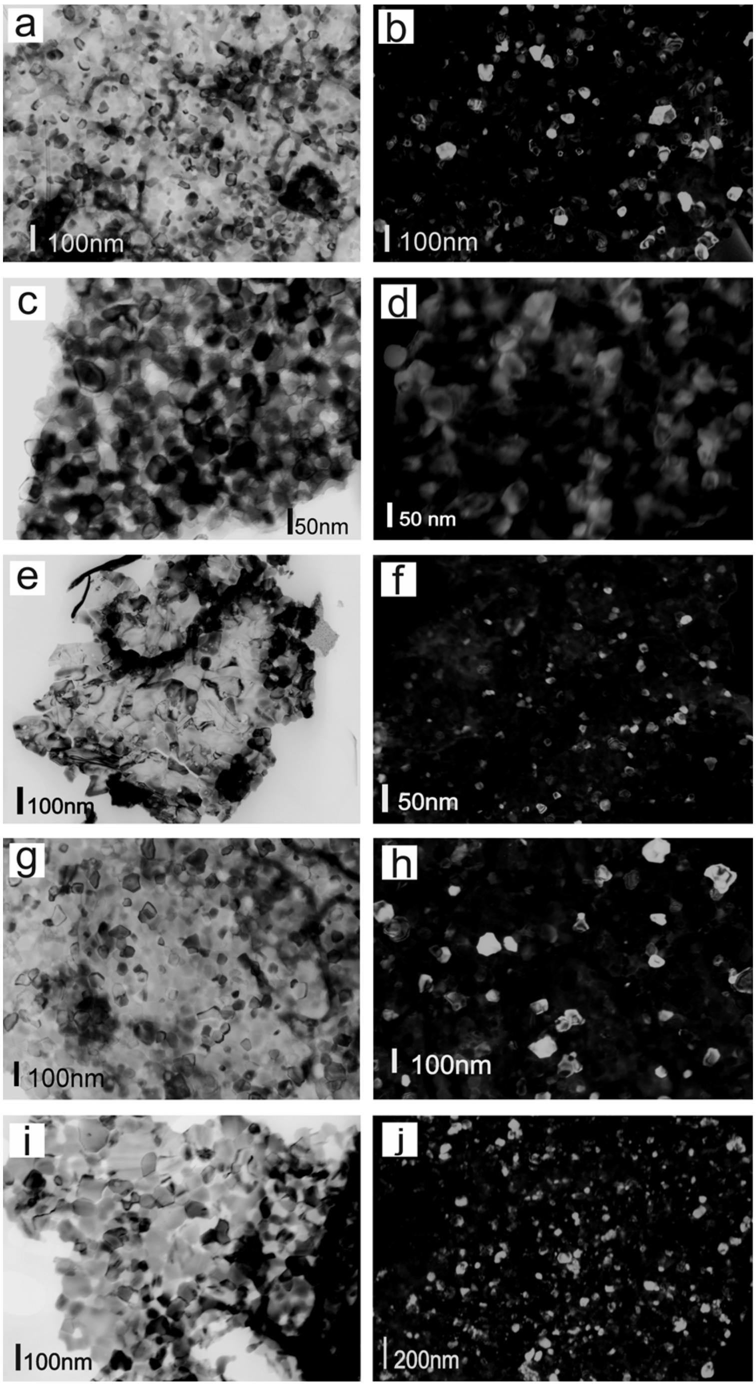

Fig. S10 TEM bright and dark field images of NPs doped with different input concentration of Zn^{2+} ions : (A, B) 2.5% (C, D) 5% (E, F) 20% (G, H) 25% (I, J) 50%.

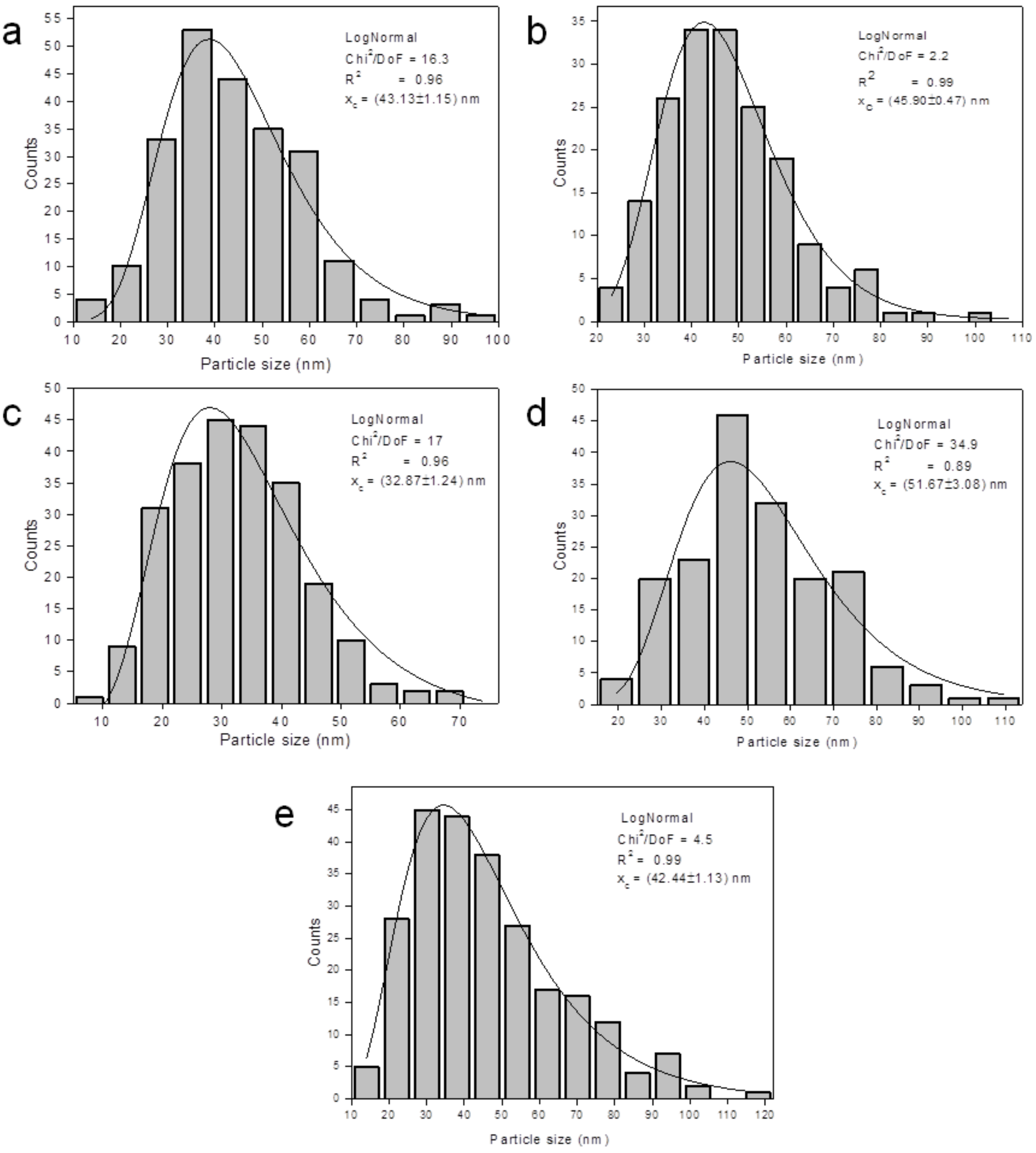

Fig. S11 Size distribution of NPs doped for different concentration of Zn^{2+} (the content of Zn^{2+} in relation to the amount of Gd^{3+} in the starting material): A) 2.5%, B) 5%, C) 20%, D) 25%, E) 50%.

Table S5. Quantum yields obtained at several different laser powers and sizes of Gd_2O_3: 1% Er^{3+}, 18% Yb^{3+} NPs, for different zinc concentrations (non-calcined samples).

The content of Zn^{2+} in relation to the amount of Gd^{3+} in the starting material	**TEM particle size (nm)**	**XRD crystallite size (nm)**	**QY (%)**	**Laser Power (mW)**
Without Zn^{2+}	-	~91	0.0235	597.7
			0.0216	289.7
			0.0188	207.4
			0.0152	188
			0.0082	68.3
			0.0054	58.3
			0.0041	42
			0.0035	37.6
			0.0014	20.5
			0.0004	14.7
2.5	~43	~76	0.0590	597.7
			0.0320	289.7
			0.0250	207.4
			0.0120	68.3
			0.0100	58.3
			0.0050	42
			0.0040	37.6
			0.0020	20.5
			0.0010	14.7
5	~ 46	~67	0.0890	597.7
			0.0210	289.7
			0.0160	207.4
			0.0080	68.3
			0.0060	58.3
			0.0030	42
			0.0030	37.6
			0.0010	20.5
20	~ 33	~80	0.0238	597.7
			0.0132	289.7
			0.0091	207.4
			0.0056	68.3
			0.0040	58.3
			0.0025	42
			0.0020	37.6
			0.0006	20.5
			0.0002	14.7
25	~ 52	~ 77	0.0170	597.7
			0.0102	289.7
			0.0087	207.4
			0.0047	68.3
			0.0040	58.3
			0.0020	42
			0.0018	37.6
			0.0006	20.5
			0.0002	14.7
50	~ 43	~67	0.0024	597.7
			0.0019	289.7
			0.0016	207.4
			0.0005	68.3
			0.0004	58.3
			0.0002	42

Table S6. Quantum yields obtained for several laser powers and sizes of Gd_2O_3: 1% Er^{3+}, 18% Yb^{3+}**,** 5% Zn^{2+} NPs, for different NaCl content.

Sample Gd_2O_3: 1%Er^{3+},18%Yb^{3+}, 5% Zn^{2+} NaCl concentration (mM)	**XRD crystallite size (nm)**	**QY (%)**	**Laser Power (mW)**
11	~81	0.0024	597.7
		0.0010	289.7
		0.0007	207.4
		0.0007	68.3
		0.0003	58.3
		0.0001	42
8	~78	0.0029	597.7
		0.0011	289.7
		0.0009	207.4
		0.0008	68.3
		0.0003	58.3
		0.0001	42
6	~75	0.0032	597.7
		0.0017	289.7
		0.0011	207.4
		0.0011	68.3
		0.0004	58.3
		0.0002	42
3	~67	0.0044	597.7
		0.0018	289.7
		0.0014	207.4
		0.0013	68.3
		0.0005	58.3
		0.0002	42

Table S7.

Gd_2O_3:1% Er^{3+}, 18% Yb^{3+}, x% Zn^{2+} (non-calcined samples)		
	Red emission (630-700 nm)	**Green emission (510 - 585 nm)**
The content of Zn^{2+} in relation to the amount of Gd^{3+} in the starting material (%)	**Number of photons absorbed per up-converted photon emitted n**	
0	2.30	no luminescence
2.5	2.21	1.57
5	2.00	1.98
20	1.88	1.94
25	2.16	(1) 0.56 (2) 2.47
50	2.17	(1) 1.82 (2) 1.54

Table S6.

Gd_2O_3:1% Er^{3+}, 18% Yb^{3+}, x% Zn^{2+} (calcined samples (2 h- 900 °C)		
	Red emission (630-700 nm)	**Green emission (510 - 585 nm)**
The content of Zn^{2+} in relation to the amount of Gd^{3+} in the starting material (%)	**Number of photons absorbed per up-converted photon emitted n**	
0	1.68	1.73
2.5	1.95	1.35
5	1.96	1.69
20	1.80	1.63
25	1.98	1.62
50	2.13	(1) 1.96 (2) 0.92

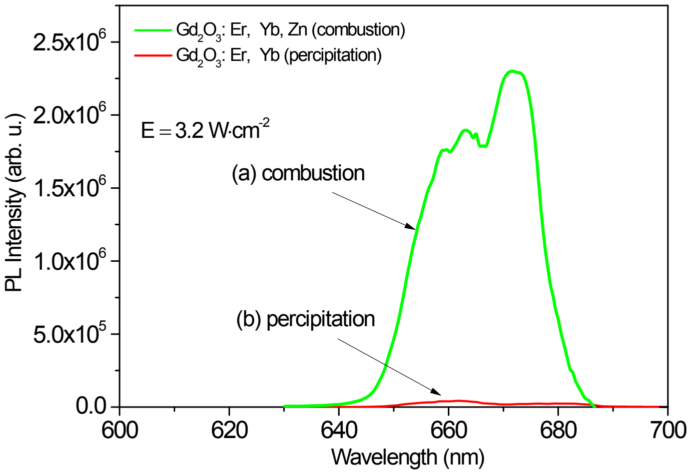

Fig. S12 Comparison of upconversion PL of Gd$_2$O$_3$:Er^{3+}, Yb^{3+}, Zn^{2+} NPs obtained by the microwave-induced solution combustion synthesis A) and the Gd$_2$O$_3$: Er^{3+}, Yb^{3+} NPs synthesized by the homogenous precipitation method B) and calcined at 900^{o}C in air by 3 h. Excitation by continues wave 980 nm laser.

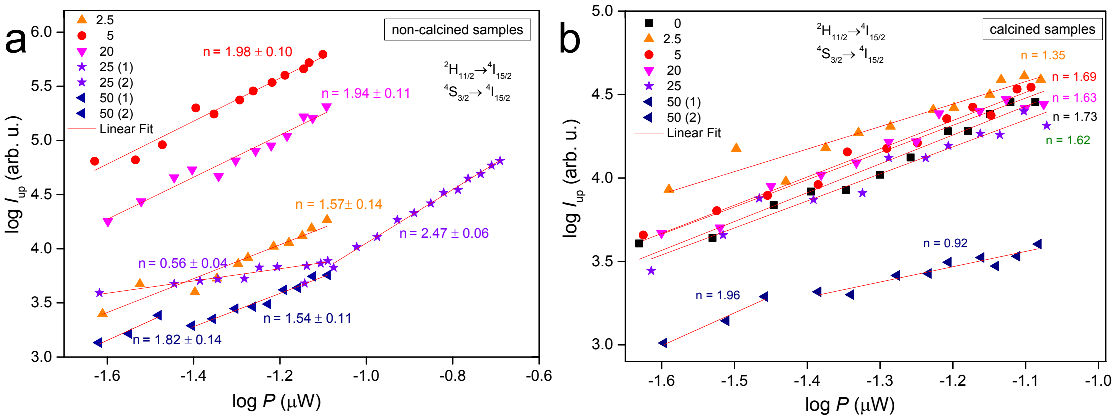

Fig. S13 Double logarithmic plots of the intensity dependencies of the up-converted fluorescence as a function of the excitation power at 980 nm (cw) for different samples A) green luminescence (non-calcined) and B) calcined samples. *n* is integer of photons absorbed in the upconversion emission process.

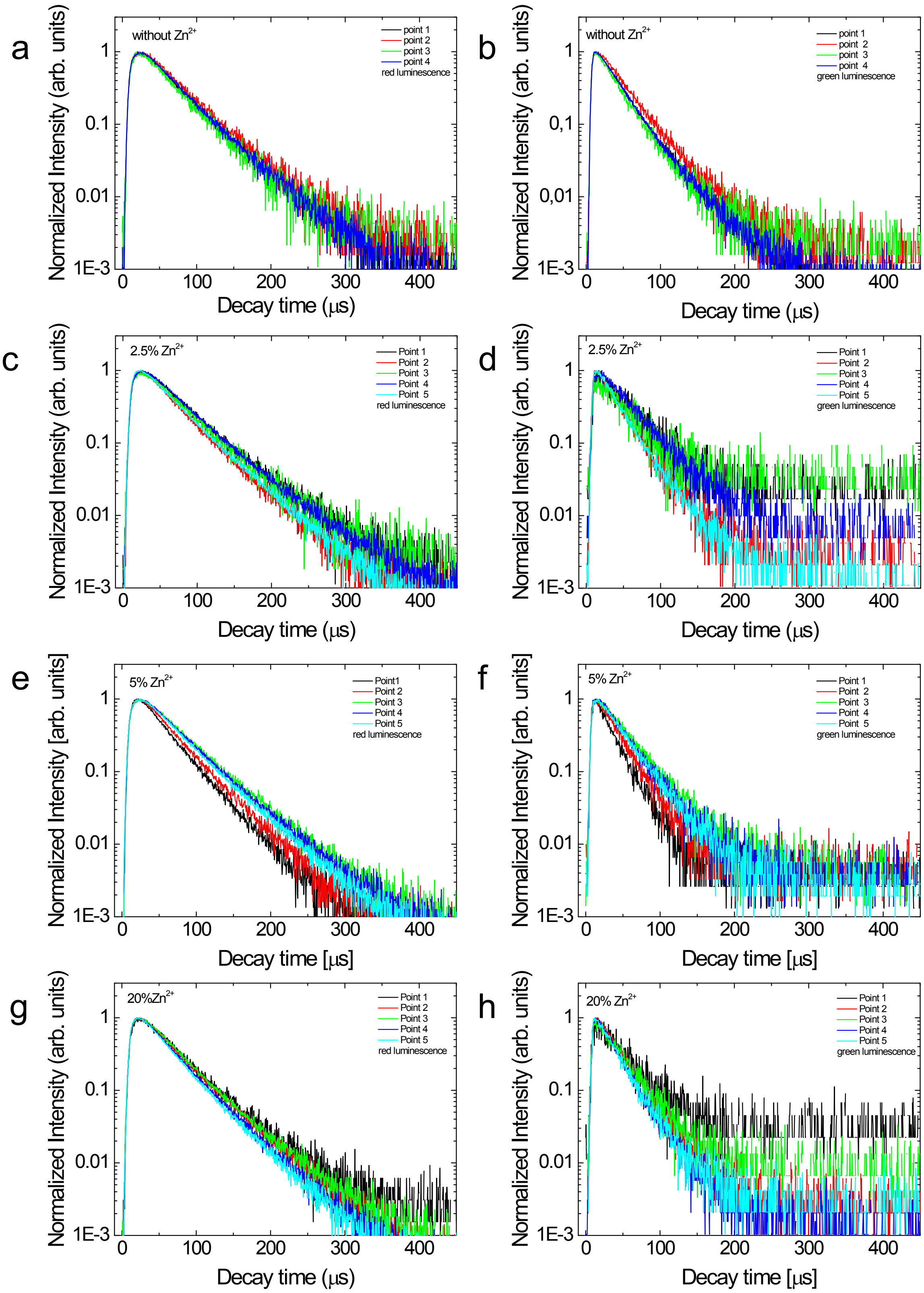

Fig. S14 Luminescence decay curves of Er^{3+} at 980 nm laser pulse for the $\lambda_{em.}$= 550 nm and $\lambda_{em.}$= 660 nm at various input content of Zn^{2+} in (A, B) 0% (C, D) 2.5% (E, F) 5% (G, H) 20%.

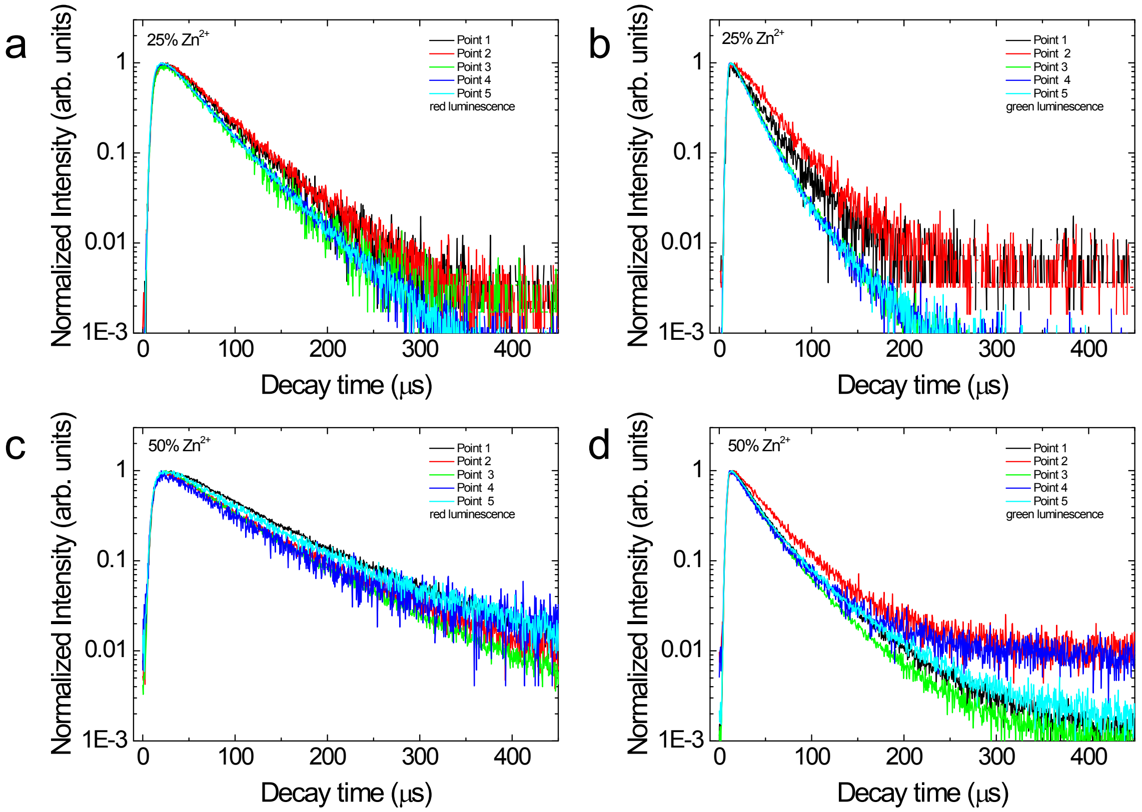

Fig. S15 Luminescence decay curves of Er^{3+} at 980 nm laser pulse for the $\lambda_{emission}$ = 550 nm and $\lambda_{emission}$ = 660 nm at various input content of Zn^{2+} in (A, B) 25% (C, D) 50%.

Table S9. Summary of the luminescence decay of sample without Zn^{2+} for the specific transitions $^4S_{3/2}\rightarrow{}^4I_{15/2}$ (green emissions) and $^4F_{9/2}\rightarrow{}^4I_{15/2}$ (red emissions).

The content of Zn^{2+} in relation to the amount of Gd^{3+} in the starting material **0%**	**Green luminescence lifetime (μs) ($^4S_{3/2} \rightarrow {}^4I_{15/2}$, 550 nm)**	**Red luminescence lifetime (μs) ($^4F_{9/2} \rightarrow {}^4I_{15/2}$, 660 nm)**
1	29.83 ± 0.10	45.45 ± 0.39
2	35.01 ± 0.24	49.07 ± 0.52
3	27.52 ± 0.17	42.92 ± 0.35
4	29.87 ± 0.11	49.45 ± 0.54

Table S10. Summary of the luminescence decay of sample with 2.5% Zn^{2+} for the specific transitions $^4S_{3/2}\rightarrow{}^4I_{15/2}$ (green emissions) and $^4F_{9/2}\rightarrow{}^4I_{15/2}$ (red emissions).

The content of Zn^{2+} in relation to the amount of Gd^{3+} in the starting material **2.5%**	**Green luminescence lifetime (µs) ($^4S_{3/2} \rightarrow {}^4I_{15/2}$, 550 nm)**	**Red luminescence lifetime (µs) ($^4F_{9/2} \rightarrow {}^4I_{15/2}$, 660 nm)**
1	44.14 ± 0.91	50.00 ± 0.30
2	30.37 ± 0.30	42.78 ± 0.19
3	47.41 ± 1.17	48.77 ± 0.31
4	39.43 ± 0.40	50.95 ± 0.28
5	27.13 ± 0.17	44.75 ± 0.19

Table S11. Summary of the luminescence decay of sample with 5% Zn^{2+} for the specific transitions $^4S_{3/2}\rightarrow{}^4I_{15/2}$ (green emissions) and $^4F_{9/2}\rightarrow{}^4I_{15/2}$ (red emissions).

The content of Zn^{2+} in relation to the amount of Gd^{3+} in the starting material **5%**	**Green luminescence lifetime (µs) ($^4S_{3/2} \rightarrow {}^4I_{15/2}$, 550 nm)**	**Red luminescence lifetime (µs) ($^4F_{9/2} \rightarrow {}^4I_{15/2}$, 660 nm)**
1	22.08 ± 0.17	36.84 ± 0.16
2	28.81 ± 0.26	42.21 ± 0.25
3	39.71 ± 0.43	49.56 ± 0.24
4	32.70 ± 0.30	48.67 ± 0.27
5	32.11 ± 0.19	45.98 ± 0.20

Table S12. Summary of the luminescence decay of sample with 20% Zn^{2+} for the specific transitions $^4S_{3/2}\rightarrow{}^4I_{15/2}$ (green emissions) and $^4F_{9/2}\rightarrow{}^4I_{15/2}$ (red emissions).

The content of Zn^{2+} in relation to the amount of Gd^{3+} in the starting material **20%**	**Green luminescence lifetime (µs) ($^4S_{3/2} \rightarrow {}^4I_{15/2}$, 550 nm)**	**Red luminescence lifetime (µs) ($^4F_{9/2} \rightarrow {}^4I_{15/2}$, 660 nm)**
1	40.48 ± 1.00	52.77 ± 0.53
2	28.91 ± 0.18	44.59 ± 0.30
3	34.07 ± 0.41	45.01 ± 0.28
4	26.74 ± 0.19	42.90 ± 0.42
5	26.66 ± 0.20	40.78 ± 0.37

Table S13. Summary of the luminescence decay of sample with 25 % Zn^{2+} for the specific transitions $^4S_{3/2}\rightarrow{}^4I_{15/2}$ (green emissions) and $^4F_{9/2}\rightarrow{}^4I_{15/2}$ (red emissions).

The content of Zn^{2+} in relation to the amount of Gd^{3+} in the starting material **25%**	**Green luminescence lifetime (µs) ($^4S_{3/2} \rightarrow {}^4I_{15/2}$, 550 nm)**	**Red luminescence lifetime (µs) ($^4F_{9/2} \rightarrow {}^4I_{15/2}$, 660 nm)**
1	29.93 ± 0.29	46.11 ± 0.30
2	35.77 ± 0.28	49.16 ± 0.30
3	22.93 ± 0.08	42.29 ± 0.36
4	22.70 ± 0.09	41.63 ± 0.21
5	22.10 ± 0.09	40.89 ± 0.21

Table S14. Summary of the luminescence decay of sample with 50% Zn^{2+} for the specific transitions $^4S_{3/2}\rightarrow{}^4I_{15/2}$ (green emissions) and $^4F_{9/2}\rightarrow{}^4I_{15/2}$ (red emissions).

The content of Zn^{2+} in relation to the amount of Gd^{3+} in the starting material **50%**	**Green luminescence lifetime (µs) ($^4S_{3/2} \rightarrow {}^4I_{15/2}$, 550 nm)**	**Red luminescence lifetime (µs) ($^4F_{9/2} \rightarrow {}^4I_{15/2}$, 660 nm)**
1	31.79 ± 0.13	86.49 ± 0.41
2	38.90 ± 0.19	72.38 ± 0.37
3	29.67 ± 0.11	67.37 ± 0.23
4	31.45 ± 0.20	72.75 ± 0.71
5	32.04 ± 0.14	81.13 ± 0.51

---

[1] Y. X. Li, W. F. Chen, X. Z. Zhou, Z. Y. Gu, Ch. M. Chen, *Materials Letters* **2005**, 59, 48–52.

[2] I. Kamińska, K. Fronc, B. Sikora, K. Koper, R. Minikayev, W. Paszkowicz, K. Sobczak, T. Wojciechowski, M. Chwastyk, A. Reszka, B. J. Kowalski, P. Stępień, D. Elbaum, *RSC Adv.*, **2014**, 4, 56596